

Supplementary Information for

Engineering a Multi-biofunctional Composite Using Poly(ethyleneimine)

Decorated Graphene Oxide for Bone Tissue Regeneration

Sachin Kumar¹, Shammy Raj¹, Kishor Sarkar², Kaushik Chatterjee^{*1}

¹Department of Materials Engineering and ²Department of Chemical Engineering

Indian Institute of Science, Bangalore 560012 India

**author to whom all correspondence should be addressed*

Email: kchatterjee@materials.iisc.ernet.in

Tel: +91-80-22933408

Table S1: XPS elemental quantification of GO, GO-g-PAA and GO_PEI

Sample	C 1s atomic (%)	N 1s atomic (%)	O 1s atomic (%)
GO	67.9	0	32.1
GO-g-PAA	59.8	0	40.2
GO_PEI	52.8	20.7	26.5

Table S2: Average roughness (Ra) measured by optical profilometry and modulus determined by DMA

Sample	Roughness (R _a) (μm)	Storage Modulus (MPa)
PCL	0.46	374 \pm 29
PCL/GO_1	0.49	421 \pm 56
PCL/GO_3	0.51	503 \pm 38
PCL/GO_5	0.51	605 \pm 43
PCL/GO_PEI_1	0.50	406 \pm 12
PCL/GO_PEI_3	0.51	435 \pm 31
PCL/GO_PEI_5	0.52	492 \pm 17

Figure S1

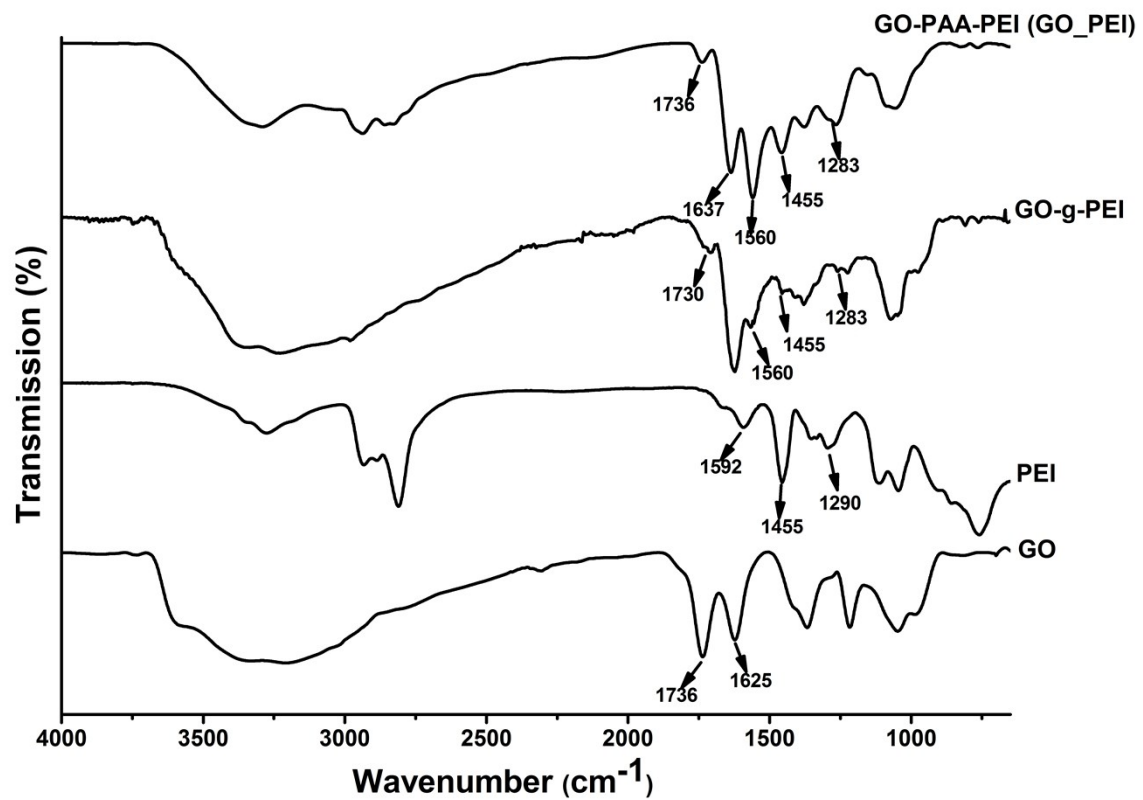


Figure S1: FTIR spectra of GO, PEI, GO-g-PEI (grafting of PEI directly on GO) and GO_PEI (PEI grafted on GO-g-PAA)

Figure S2

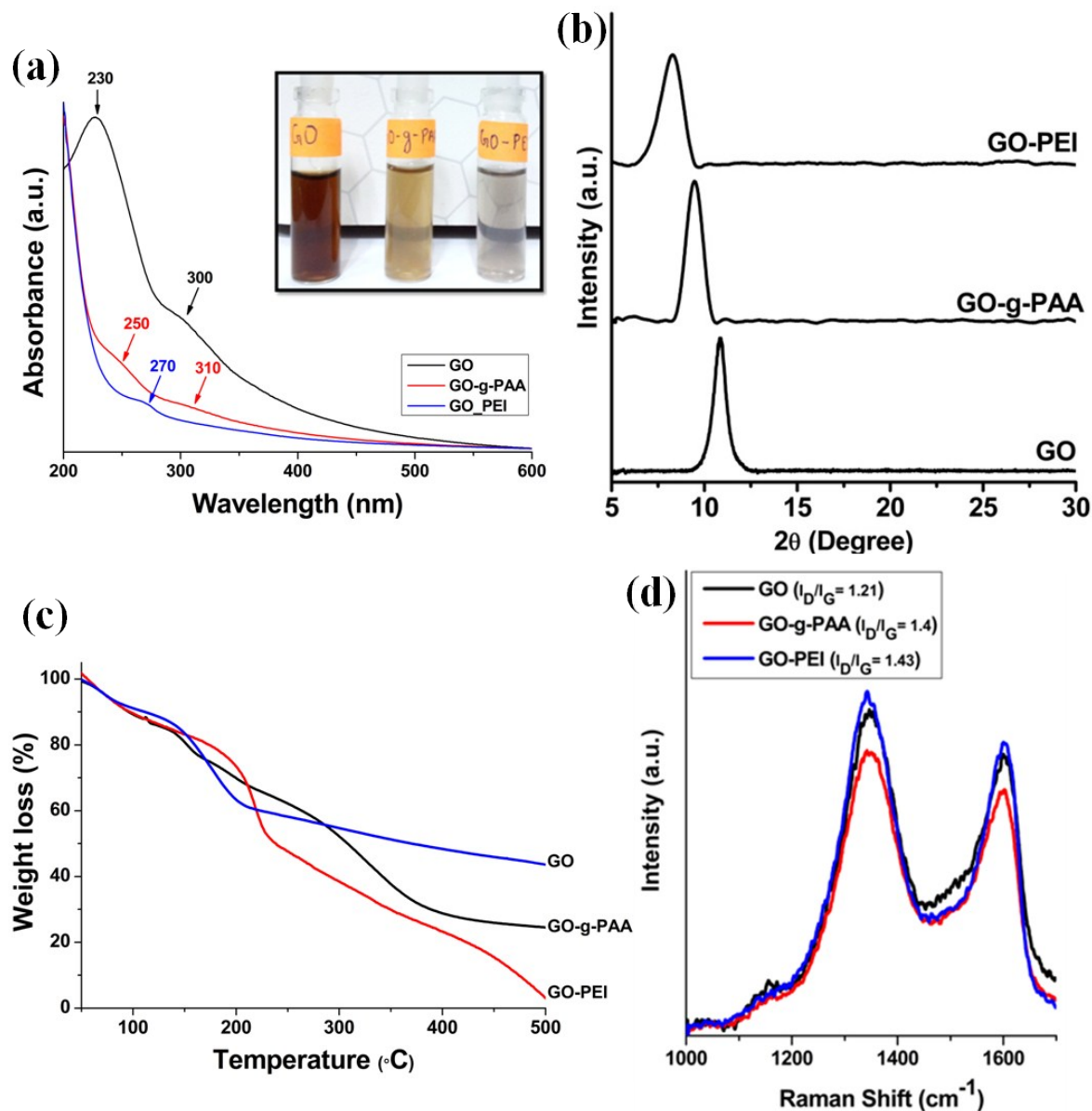


Figure S2: (a) UV-Vis spectra with inset showing digital photographs of aqueous dispersions of GO, GO-g-PAA and GO-PEI nanoparticles (b) XRD profiles of GO, GO-g-PAA and GO-PEI nanoparticles, (c) TGA thermographs of GO, GO-g-PAA and GO-PEI and (d) Raman spectra of GO, GO-g-PAA and GO-PEI

Figure S3

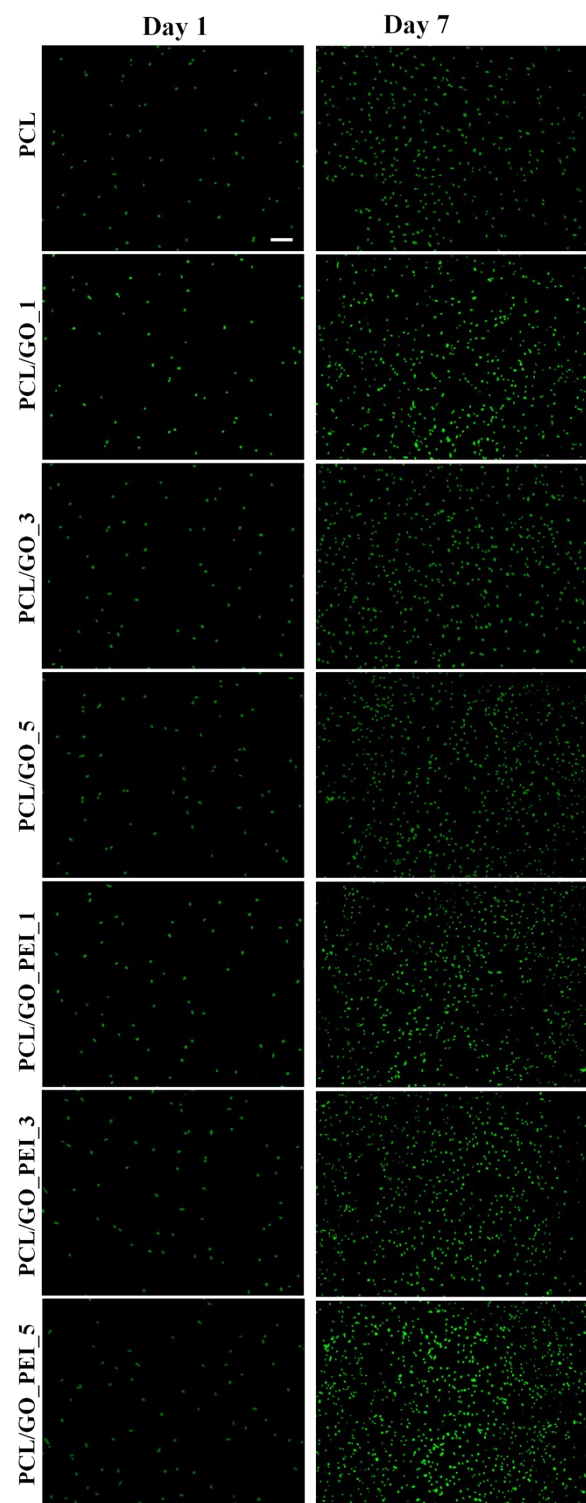


Figure S3: Fluorescence micrographs of stained nuclei of hMSCs at days 1 and 7 on neat PCL and its different composites (scale bar = 200 μm) (False colored with green for DAPI for enhanced clarity)

Figure S4

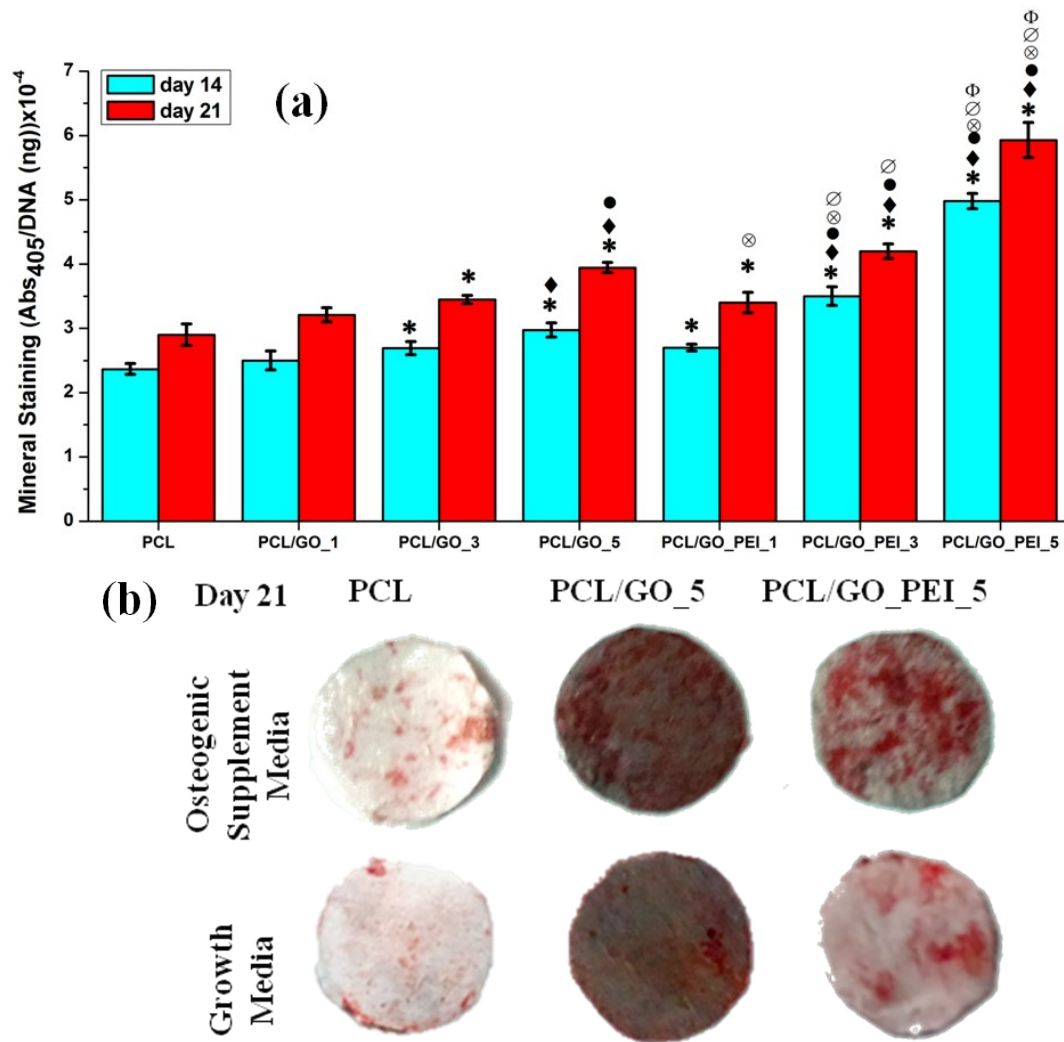


Figure S4: (a) Mineralization of hMSCs on PCL and its different composites in the presence of osteogenic supplements as day 14 and 21 and (b) representative digital photographs of ARS stained (red) surfaces of PCL, PCL/GO_5 and PCL/GO_PEI_5 films at day 21 in the presence and absence of osteogenic supplements. Statistically significant differences ($p < 0.05$) compared to PCL, PCL/GO_1, PCL/GO_3, PCL/GO_5, PCL/GO_PEI_1 and PCL/GO_PEI_3, are indicated by *, ◆, ●, ⊗, ⊖ and Φ, respectively.

Figure S5

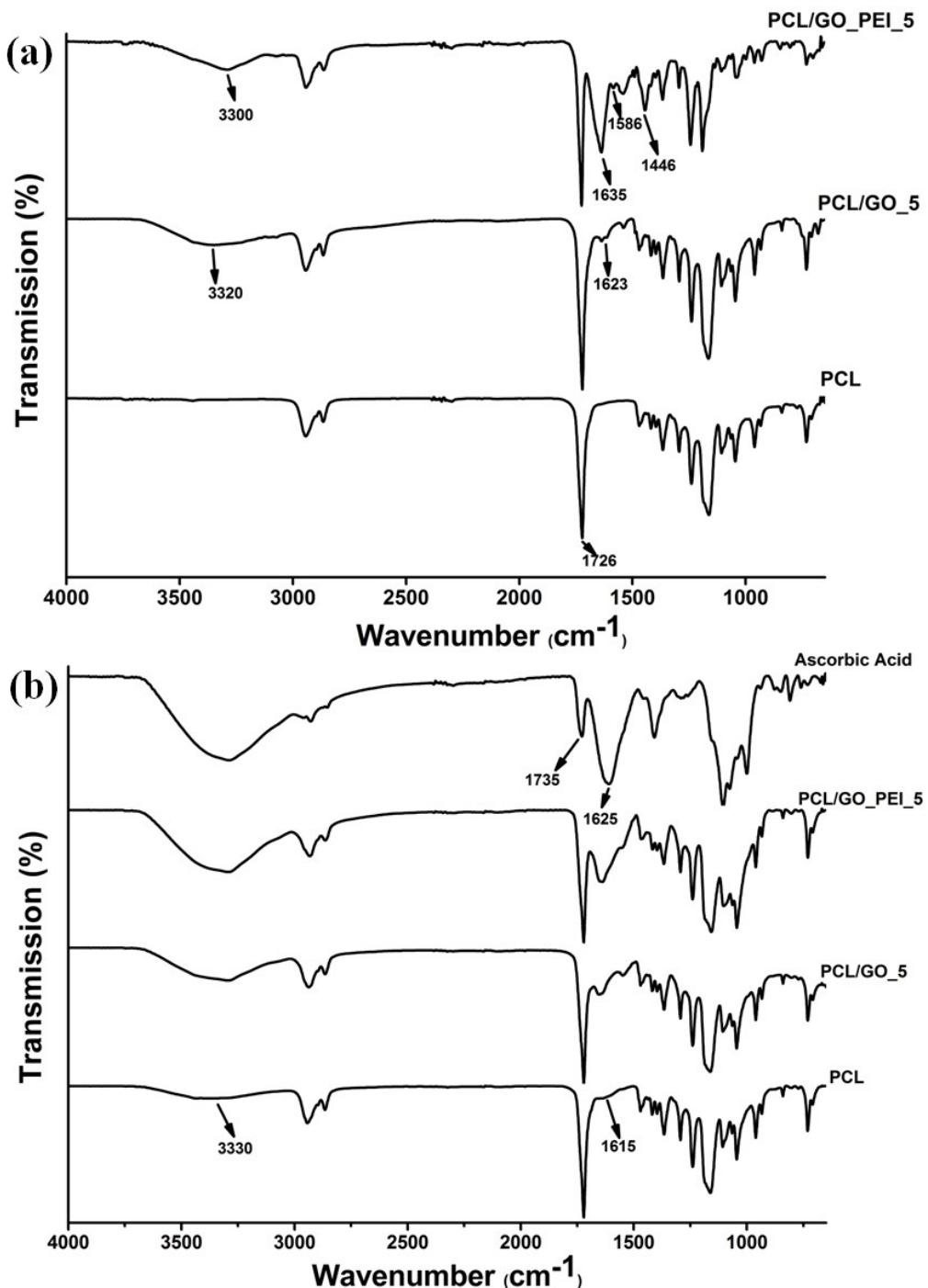


Figure S5: Attenuated total reflection mode FTIR (ATR-FTIR) spectra of PCL, PCL/GO_5 and PCL/GO_PEI_5 before (a) and after (b) adsorption of ascorbic acid for 3 days. Neat PCL film showed intense peak at 1726 cm^{-1} that may be attributed to the ester group of PCL. PCL/GO_5 composite showed the peaks for PCL along with two additional peaks at 3320 cm^{-1} and 1623 cm^{-1} arising from $-\text{OH}$ and $\text{C}=\text{C}$ vibration of aromatic chains on GO. PCL/GO_PEI_5 showed all the peaks for PCL along with few new peaks at 3300 cm^{-1} , 1635 cm^{-1} , 1586 cm^{-1} and 1446 cm^{-1} corresponding to the $-\text{OH}$, $-\text{NH}$ and $-\text{CH}$ groups from

GO_xPEI. These new peaks in PCL/GO_x and PCL/GO_xPEI composites films confirm the presence of GO and GO_xPEI particles in PCL matrix.

The spectra for ascorbic acid showed broad –OH stretching peak at 3325 cm⁻¹. Peaks at 1735 cm⁻¹ and 1625 cm⁻¹ can be attributed C=O and C=C vibrational stretching from the five-membered lactone ring of ascorbic acid. The PCL film after adsorption showed peaks at 3330 cm⁻¹ and 1615 cm⁻¹ which were absent for neat PCL. Ascorbic acid adsorbed on PCL/GO_x showed intense and broad –OH stretching peak. Furthermore, the peak at around 1630 cm⁻¹ also became intense in comparison to the PCL/GO_x surface without ascorbic acid. Ascorbic acid adsorbed on PCL/GO_xPEI composites showed much more intense and broader peaks among all the three samples at 3320 cm⁻¹ and 1635 cm⁻¹. PCL/GO and PCL/GO_xPEI composites showing intense and broadness in peaks at 3330 cm⁻¹ and 1635 cm⁻¹ similar to that of ascorbic acid suggesting adsorption of ascorbic acid increases due to hydrogen bonding with GO and GO_xPEI. Intermolecular interaction through hydrogen bonds generally leads to broadening and stronger –OH stretching intensity. Thus, ATR-FTIR further confirms more surface adsorption of ascorbic acid on PCL/GO_x and PCL/GO_xPEI composites.

Figure S6

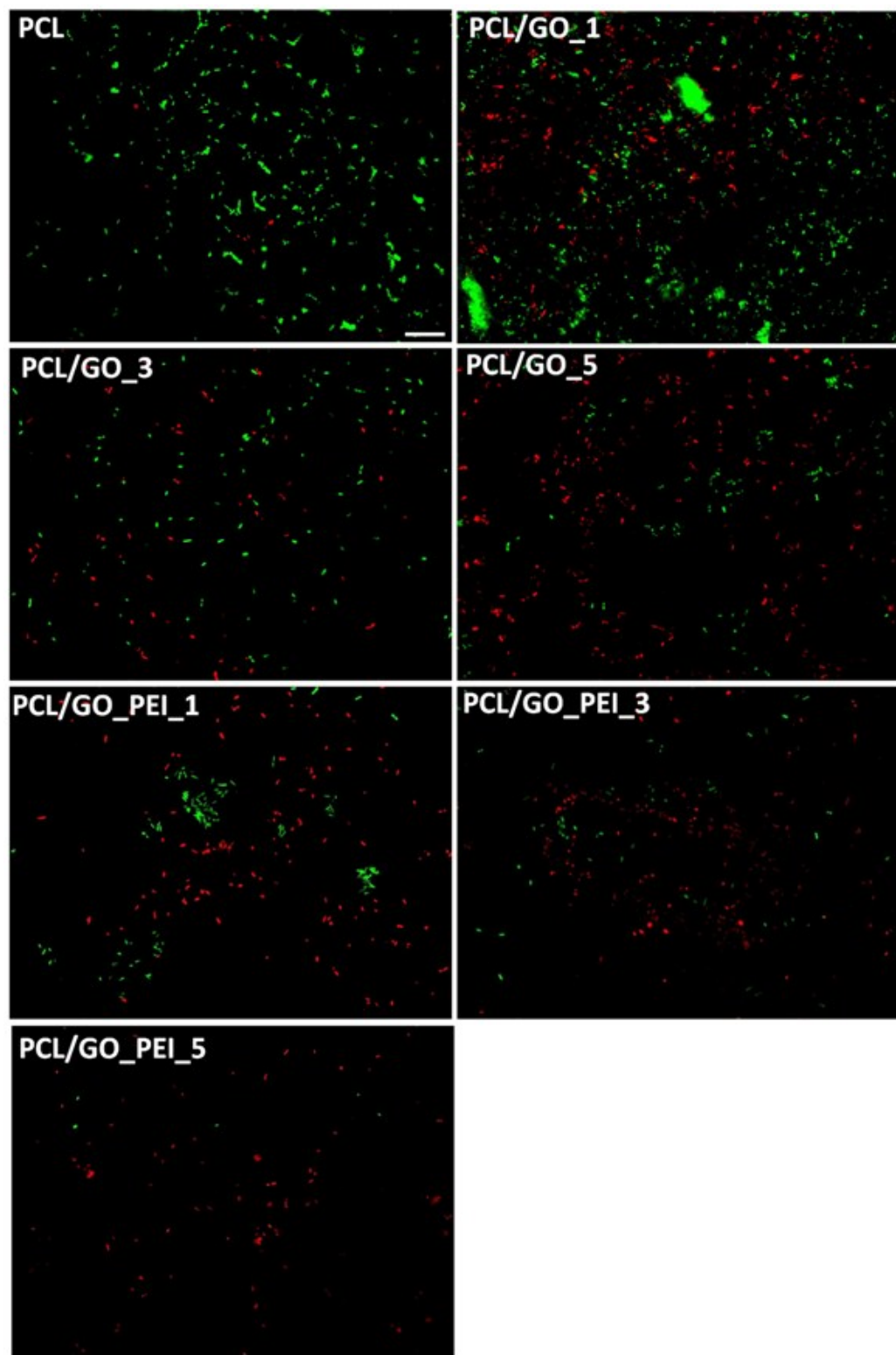


Figure S6: Fluorescence micrographs of *E. coli* stained for live/dead imaging on PCL and the different composites (scale bar = 25 μ m)

Figure S7

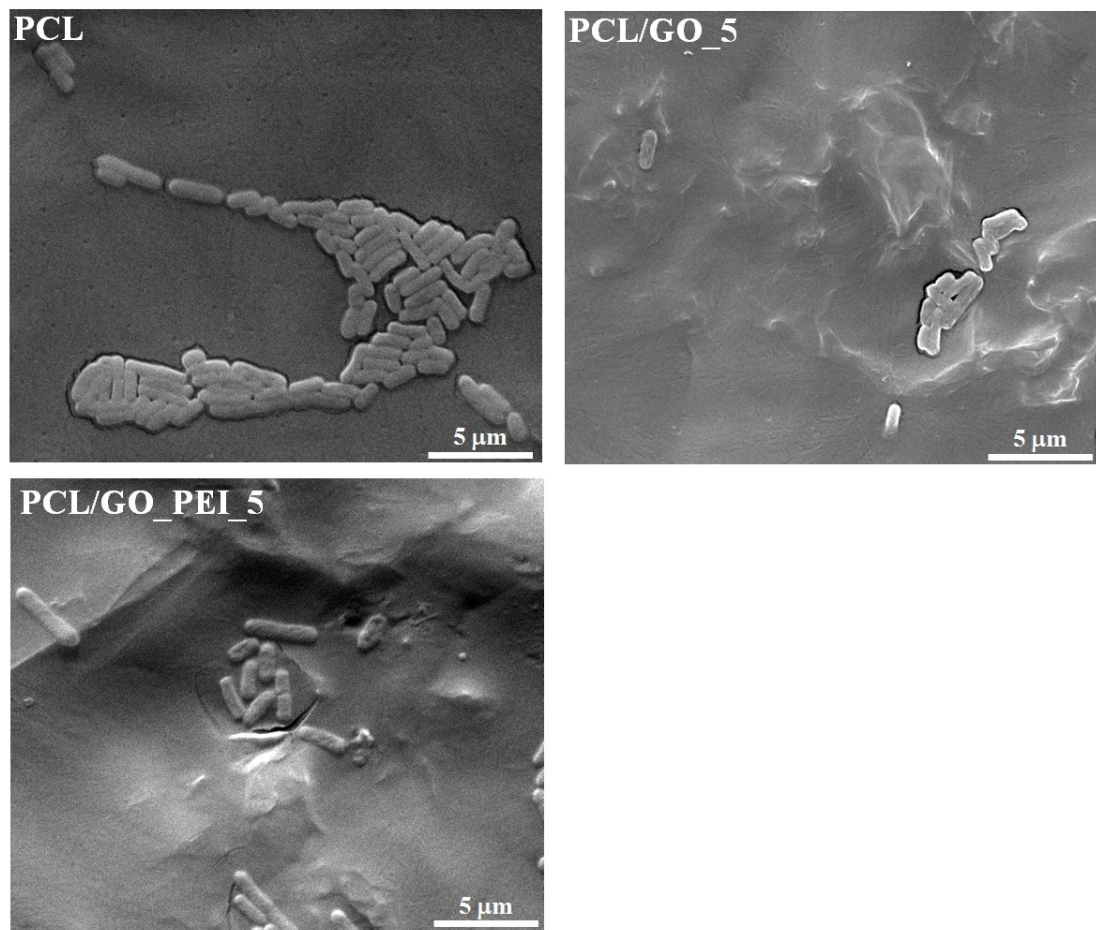


Figure S7: SEM micrographs of bacterial cells on PCL, PCL/GO_5 and PCL/GO_PEI_5